ARTICLE

Theoretical Analysis on Fully Differential Cross-Sections for C^{6+} Single Ionization of Helium

Hui-xiao Duan, Shi-yan Sun, Xiao-ying Fang, Rui-fang Zhang, Xiang-fu Jia*

Center for Molecular Research, School of Physics and Information Engineering, Shanxi Normal University, Linfen 041004, China

(Dated: Received on November 27, 2013; Accepted on January 10, 2014)

The four-body model has been used to calculate the fully differential cross-sections (FDCS) for the single ionization of helium by 100 MeV/amu C^{6+} impact in geometries. By comparing with experimental data and other theories, we find the results of four-body model are in very good agreement in the scattering plane, but poor agreement out of the scattering plane. Accordingly, the contributions of different scattering amplitudes to FDCS are analyzed. It is found that the cross sections due to the interference of the scattering amplitudes between projectile-target nucleus interaction and projectile-ejected electron interaction almost tend to experimental results around the recoil region in geometries. In particular in the perpendicular plane, the cross section originating from interference of the scattering amplitudes between projectile-target nucleus and projectile-ejected electron interactions yields an experimental double-peak structure in the angular distribution. However, this feature could not be presented by the interference of the three amplitudes. Thus, the failure of the four-body model predicting the feature in this geometry may be attributed to an inappropriate weighting of the three amplitudes.

Key words: Ion-impact ionization, Fully differential cross section, Four-body model, Interference effect

I. INTRODUCTION

Ion-atom collisions have been a field of intense activity in atomic physics, but experimental results for single ionization processes occurring in heavy ion-atom collisions are still not fully understood [1, 2]. In particular, the measurements of the fully differential cross sections (FDCS) in geometries other than the scattering plane [3] have not been explained [4, 5].

For a very small perturbation it was generally expected that even the relatively simple first-born-approximation (FBA) [4] gave reasonably good results at such high impact energies (100 MeV/amu) for all geometries. Indeed, in the scattering plane the FBA calculations yielded good agreement, however, poor agreement for outside the scattering plane, especially in the perpendicular plane the FBA results totally disagree with the experiment both qualitatively and quantitatively. Other relatively senior perturbative models, such as the three-body distorted-wave (3DW) model [6] and the continuum distorted wave (CDW) approximation [3, 7], also cannot give a satisfying result in the perpendicular plane. For nonperturbative theories such as the fully quantum-mechanical convergent close-coupling (CCC) approach [5] and the coupled-pseudostate (CP) approach [4, 8], neither of them eliminated the discrepancy with experiment in the perpendicular plane. A time-dependent close-coupling (TDCC) [9] approach, led to a perpendicular plane FDCS with the positions of the peaks in better agreement with experiment. However, the magnitude of the FDCS remained considerably lower than the experiment.

So far none of the published theoretical investigations has been able to obtain reasonable agreement with the measured angular distribution of the ejected electron in the perpendicular plane. Accordingly, further theoretical analysis and calculations are appropriate and interesting.

In this work, we use a simple four-body model, which has been employed in the fields of electron-atom [10] and ion-atom collisions [11, 12], to analyze the FDCS for single ionization of helium by 100 MeV/amu C^{6+} impact. Also the importance of interference effects in determining the shape of the FDCS is demonstrated, specifically, we discuss in detail the contribution of scattering amplitudes to FDCS in the scattering and perpendicular planes. In the present model, the four-body initial state is represented as a product of the plane wave for the projectile and the Hartree Fock (HF) ground-state wave function of helium. The final state is approximated as a product of the He^+ ground-state wave function for passive electron and three-Coulomb wave. The four-body

*Author to whom correspondence should be addressed. E-mail: jiaxf@dns.sxnu.edu.cn, Tel.: +86-357-2051189

cross sections were compared with the corresponding experimental results and the ability of the present model to reproduce the peak structure of the experimental data was assessed.

II. THEORY

We consider single ionization of helium by the impact of C^{6+} with incident momentum $\mathbf{K}_i$ relative to the atomic center of mass. In the center-of-mass (CM) system, the T-matrix is defined as

$$T_{fi} = \langle \psi_f^-(\mathbf{r}_1, \mathbf{r}_\mathrm{T}, \mathbf{R}_\mathrm{P}) | V_i | \Phi_i^+(\mathbf{r}_1, \mathbf{r}_\mathrm{T}, \mathbf{R}_\mathrm{P}) \rangle \quad (1)$$

where $\mathbf{r}_1$ is the coordinate of the passive electron relative to the target nucleus. $\mathbf{r}_\mathrm{T}$ represents the coordinates of the ionized electron with respect to the target ion. $\mathbf{R}_\mathrm{P}$ is the position of the projectile relative to the atomic center of mass.

The perturbation V_i corresponding to the initial state is given as:

$$\begin{aligned} V_i &= V_\mathrm{PT} + V_\mathrm{Pe} + V_\mathrm{Pe1} \\ &= \frac{Z_\mathrm{P} Z_\mathrm{T}}{R} - \frac{Z_\mathrm{P}}{\mathbf{r}_\mathrm{P}} - \frac{Z_\mathrm{P}}{|\mathbf{R} - \mathbf{r}_1|} \end{aligned} \quad (2)$$

here Z_P and Z_T are the chares of the projectile and target nucleus, respectively, R represents the position of the projectile with respect to the target nucleus, r_P represents the coordinates of the ionized electron with respect to the projectile. Hence, Eq.(1) may be rewritten as:

$$\begin{aligned} T_{fi} &= T_\mathrm{PT} + T_\mathrm{Pe} + T_\mathrm{Pe1} \\ &= \langle \psi_f^- | V_\mathrm{PT} | \Phi_i^+ \rangle + \langle \psi_f^- | V_\mathrm{Pe1} | \Phi_i^+ \rangle + \\ &\quad \langle \psi_f^- | V_\mathrm{Pe1} | \Phi_i^+ \rangle \end{aligned} \quad (3)$$

$$T_\mathrm{P,core} = T_\mathrm{PT} + T_\mathrm{Pe1} \quad (4)$$

here T_PT, T_Pe, and T_Pel represent T-matrix elements, which is the interaction of the incoming projectile with the target nucleus, the ejected electron, and passive electron, respectively. $T_\mathrm{P,core}$ represents the coherent sum of the scattering amplitudes T_PT and T_Pel.

The four-body initial state wave function

$$\Phi_i^+(r_1, r_\mathrm{T}, \mathbf{R}_\mathrm{P}) = \left(\frac{1}{2\pi}\right)^{3/2} \exp(i\mathbf{K}_i \cdot \mathbf{R}_\mathrm{P}) \phi_i(r_1, r_\mathrm{T}) \quad (5)$$

In the present calculation, we choose the analytical fitting to the HF wave function given by Byron and Joachain [13] to describe $\phi_i(r_1, r_\mathrm{T})$,

$$\phi_i(r_1, r_\mathrm{T}) = U(r_1) U(r_\mathrm{T}) \quad (6)$$

$$U(r) = (4\pi)^{-1/2} (A\mathrm{e}^{-\alpha r} + B\mathrm{e}^{-\beta r}) \quad (7)$$

where A=2.60505, B=2.08144, α=1.41, and β=2.61.

The four-body final state wave function is represented as

$$\psi_f^-(\mathbf{r}_1, \mathbf{r}_\mathrm{T}, \mathbf{R}_\mathrm{P}) = \phi_f(\mathbf{r}_1) \psi_\mathrm{3C}^-(\mathbf{r}_\mathrm{T}, \mathbf{R}_\mathrm{P}) \quad (8)$$

The three Coulomb wave ψ_3C^- can be expressed as [14]

$$\begin{aligned} \psi_\mathrm{3C}^- &= N \exp(i\mathbf{k}_\mathrm{T} \cdot \mathbf{r}_\mathrm{T}) \exp(i\mathbf{K}_\mathrm{P} \cdot \mathbf{R}_\mathrm{P}) \\ &\quad \times {}_1\mathrm{F}_1(i\alpha_\mathrm{Te}; 1; -i(k_\mathrm{T} r_\mathrm{T} + \mathbf{k}_\mathrm{T} \cdot \mathbf{r}_\mathrm{T}) \\ &\quad \times {}_1\mathrm{F}_1(i\alpha_\mathrm{PT}; 1; -i(K_\mathrm{P} R_\mathrm{T} + \mathbf{K}_\mathrm{P} \cdot \mathbf{R}_\mathrm{T}) \\ &\quad \times {}_1\mathrm{F}_1(i\alpha_\mathrm{Pe}; 1; -i(k_\mathrm{P} r_\mathrm{P} + \mathbf{k}_\mathrm{P} \cdot \mathbf{r}_\mathrm{P}) \end{aligned} \quad (9)$$

The $\mathbf{K}_\mathrm{P}$ and $\mathbf{k}_\mathrm{T}$ are the momentums of scattered projectile and ejected electron, respectively, which are both considered with respect to He^+.

N is a normalization factor given by

$$\begin{aligned} N &= (2\pi)^{-3} \Gamma[(1 - i\alpha_\mathrm{Te})(1 - i\alpha_\mathrm{PT})(1 - i\alpha_\mathrm{Pe})] \cdot \\ &\quad \exp\left[-\frac{1}{2}\pi(\alpha_\mathrm{Te} + \alpha_\mathrm{PT} + \alpha_\mathrm{Pe})\right] \end{aligned} \quad (10)$$

where ${}_1F_1$ and Γ are the confluent hypergeometric function and gamma function, respectively. The Sommerfeld parameters have the form

$$\alpha_\mathrm{Te} = -\frac{\mu_\mathrm{Te} Z_\infty}{k_\mathrm{T}} \quad (11)$$

$$\alpha_\mathrm{PT} = \frac{\mu_\mathrm{PT} Z_\mathrm{P} Z_\infty}{K_\mathrm{P}} \quad (12)$$

$$\alpha_\mathrm{Pe} = -\frac{\mu_\mathrm{Pe} Z_\mathrm{p}}{k_\mathrm{P}} \quad (13)$$

here, μ_Pe and μ_PT are the reduced masses of the projectile-ionized electron subsystems and projectile-target, respectively.

Thus, the FDCS is given as follows [15, 16]:

$$\frac{\mathrm{d}^3\sigma}{\mathrm{d}\Omega_\mathrm{P} \mathrm{d}\Omega_\mathrm{e} \mathrm{d}E_\mathrm{e}} = N_\mathrm{e} (2\pi)^4 \mu_\mathrm{Te} \mu_\mathrm{P,He}^2 \frac{K_\mathrm{P} k_\mathrm{T}}{K_i} |T_{fi}|^2 \quad (14)$$

here N_e is the number of electrons in the atomic shell, $\mathrm{d}\Omega_\mathrm{P}$ and $\mathrm{d}\Omega_\mathrm{e}$ denote the differential solid angles with respect to $\mathbf{K}_\mathrm{P}$ for the scattered projectile and the ionized electron, respectively, while $\mathrm{d}E_\mathrm{e}$ represents the energy interval of the ejected electron. μ_Te is the reduced mass of the ionized electron-target ion subsystem, $\mu_\mathrm{P,He}$ is the reduced mass of the projectile-atom system. An uncertain point of this model represents the use of the asymptotic charge Z_∞=1.

If we switch off both the projectile-target ion and the projectile-ionized electron interactions (α_Pe=α_PT=0) in the Eq.(8), the result takes on the form of the FBA,

$$\begin{aligned} \Psi_\mathrm{f1C}^- &= \varphi_f(\mathbf{r}_1)(2\pi)^{-3} \exp(i\mathbf{K}_\mathrm{P} \cdot \mathbf{R}_\mathrm{P} + i\mathbf{k}_\mathrm{T} \cdot \mathbf{r}_\mathrm{T}) \cdot \\ &\quad \exp\left(-\frac{1}{2}\pi\alpha_\mathrm{Te}\right) \Gamma(1 + i\alpha_\mathrm{Te}) \cdot \\ &\quad {}_1\mathrm{F}_1[i\alpha_\mathrm{Te}; 1; -i(k_\mathrm{T} r_\mathrm{T} + \mathbf{k}_\mathrm{T} \cdot \mathbf{r}_\mathrm{T})] \end{aligned} \quad (15)$$

DOI:10.1063/1674-0068/27/03/279-284

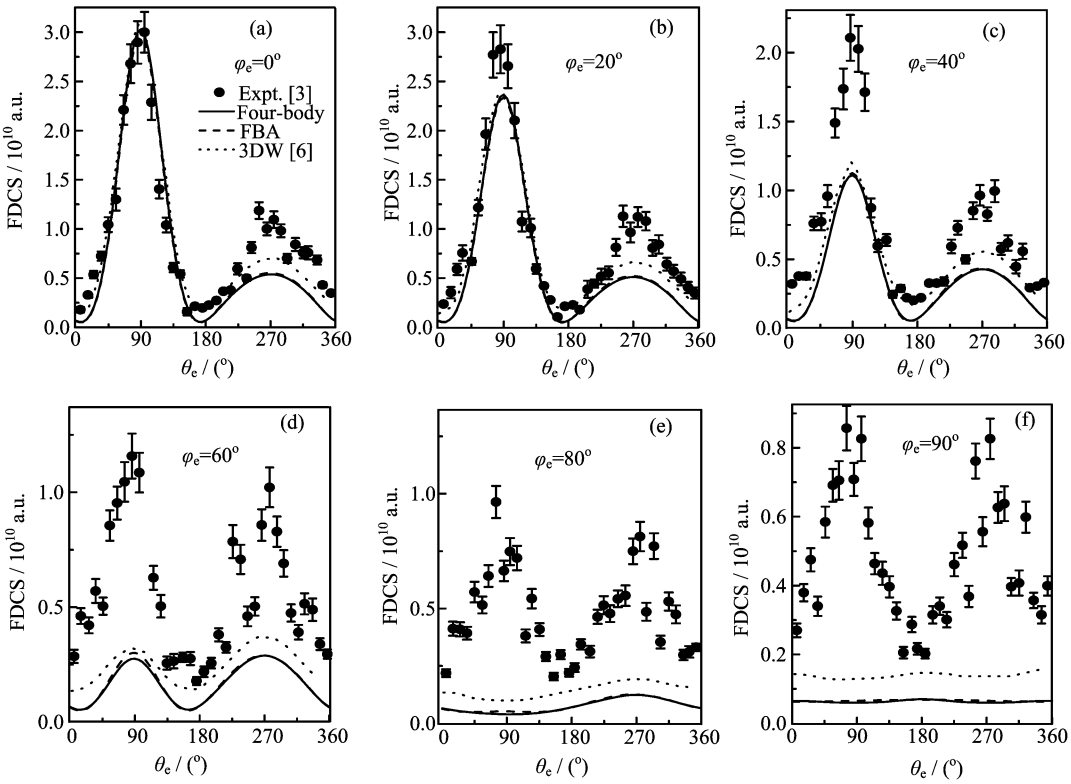

FIG. 1 FDCS in different geometries for 100 MeV/amu C^{6+} single ionization of helium with the ejected electron energy of 6.5 eV and the momentum transfers of 0.75 a.u. The angle θ_e is the emission angle of the electron. The cross sections are presented in the laboratory frame system, the laboratory frame system conversion from CM to laboratory multiply by a factor of 16 [7].

It is worth noting that in the 3DW approximation, helium atom is treated as a hydrogenlike atom, so the projectile-passive electron interaction is not considered in the perturbation. The description of the final-state wave function for the ejected electron is also different. In the four-body calculation, the wave function for the ejected electron is a Coulomb wave. Whereas in the 3DW approximation, it is a numerical solution of the HF Schrödinger equation.

The nine-dimensional integral (Eq.(1)) can be reduced analytically, and without any further approximation, to a two-dimensional integral on the real parameters [11], which has to be carried out numerically.

III. RESULTS AND DISCUSSION

We have computed the FDCS, by Eq.(14), for single ionization of helium by C^{6+} ion at incident energy of 100 MeV/amu in geometries. Calculations made at an ejected electron energy of 6.5 eV and a momentum transfer of 0.75 a.u. correspond to the measurements of Schulz *et al.* [3] for various ejected electron azimuthal angles φ_e, which ranges from 0° to 90°. The results are presented in Fig.1. The 3DW and FBA theoretical results are also provided for comparison.

From Fig.1, it is clearly seen that the positions of experimental peaks at emission angle θ_e of 90° and 270° do not change in all geometries. We note that φ_e=0° (Fig.1(a)) corresponds to the scattering plane. In the scattering plane, the four-body, FBA, and 3DW models have similar results, and the three theoretical results are in excellent agreement with the experimental data around the binary peak. However, there is some deviation near the recoil peak, the cross sections of the theories are smaller than the measurement.

As φ_e increases, the binary peak drops for both the experiment and theory, but the decrease in the binary peak is quicker for the theories. Moreover, the difference of theoretical calculations from the experimental data increases and becomes significant at φ_e=40° (Fig.1(c)). At φ_e=60°, both the binary peak and the recoil peak are roughly equal in magnitude. When φ_e=80°, the theoretical maximum disappears and exhibits a dip near 90°, however, the experimental binary peak remains a peak. φ_e=90° (Fig.1(f)) corresponds to the perpendicular plane. It is clearly seen that the experimental FDCS is symmetric about θ_e=180°, and has two well-pronounced peaks near 90° and 270°. However, there are some marked discrepancies between experiment and theoretical results both in terms of intensity and in terms of shape. The four-body and 3DW mod-

DOI:10.1063/1674-0068/27/03/279-284

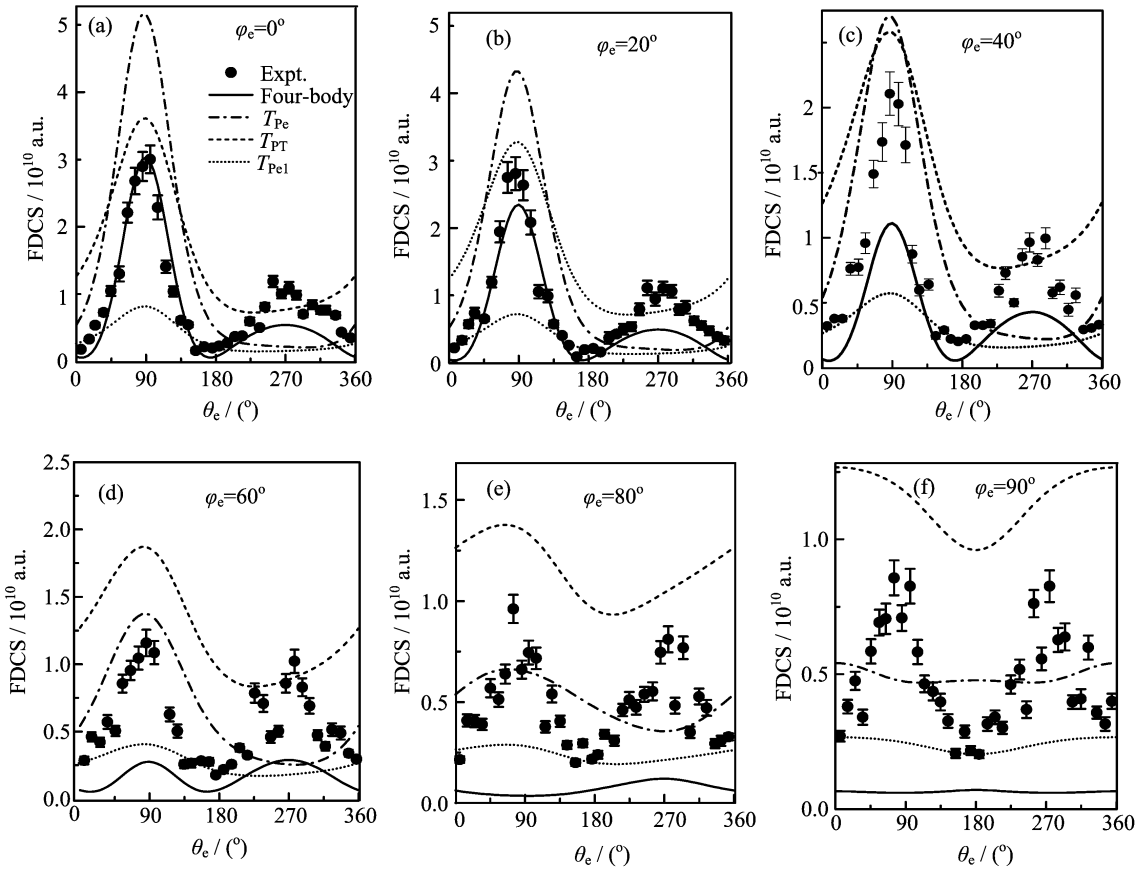

FIG. 2 The incoherent contributions to the FDCS of the scattering amplitudes.

els produce two shallow minima. The cross sections of four-body and 3DW models have a one-peak structure with the maximum near 180°, but we find a minimum in the experimental data. FBA yields a flat angular distribution. In general, there is a considerable discrepancy between the theoretical results and the measurements in the perpendicular plane.

In the experimental data, the magnitude of the recoil peak does not change dramatically, but the recoil peak gets less pronounced in all theories. Figure 1 clearly presents the difference between experiment and theory in all geometries, as angle φ_e increases, the disagreement of theoretical results with experiment becomes more significant. In fact, except for φ_e=80° and φ_e=90°, the FBA has reproduced peak-structure of experiment. The four-body theory does not show its superiority to the 3DW and FBA models. Therefore, it can draw conclusion that as φ_e is increased from 0° to 60° the four-body effect is not obvious. At φ_e=80° and φ_e=90° all theoretical results are in very bad agreement with experimental data.

Figure 1 clearly shows the deterioration of agreement between experimental data and theoretical results from scattering plane to perpendicular plane. It is obvious that the present theory based on a four-body model does not give a significant improvement over a three-body model. In fact, most of the existing theoretical methods, such as CCC [5] and CP [8] approaches, also do not reproduce the experimental structure in out-of-plane geometries. Therefore, this is still a challenge for our theoretical workers, especially for the perpendicular plane.

To explore the physical origin of the peak structure in the FDCS, we examine the contributions of different scattering amplitudes to the FDCS of the present four-body model. According to Eq.(3), calculation results are displayed in Fig.2 and Fig.3. The contributions of the three individual scattering amplitudes to the cross-sections are presented in Fig.2. Figure 3 shows the contributions arising from $T_{P,core}$ and interference between T_{PT} and T_{Pe}.

In the scattering plane (Fig.2(a)), the major individual incoherent contribution to the cross-section around the binary region comes from the scattering amplitude T_{Pe} (*i.e.*, postcollisional interaction between the projectile and ionized electron [17]). As shown in the figure, the individual incoherent contribution arising from T_{Pe1} is the smallest, so scattering amplitude T_{Pe1} may be neglected in the calculations. Figure 3(a) shows, the destructive interference between T_{PT} and T_{Pe} leads to the

DOI:10.1063/1674-0068/27/03/279-284

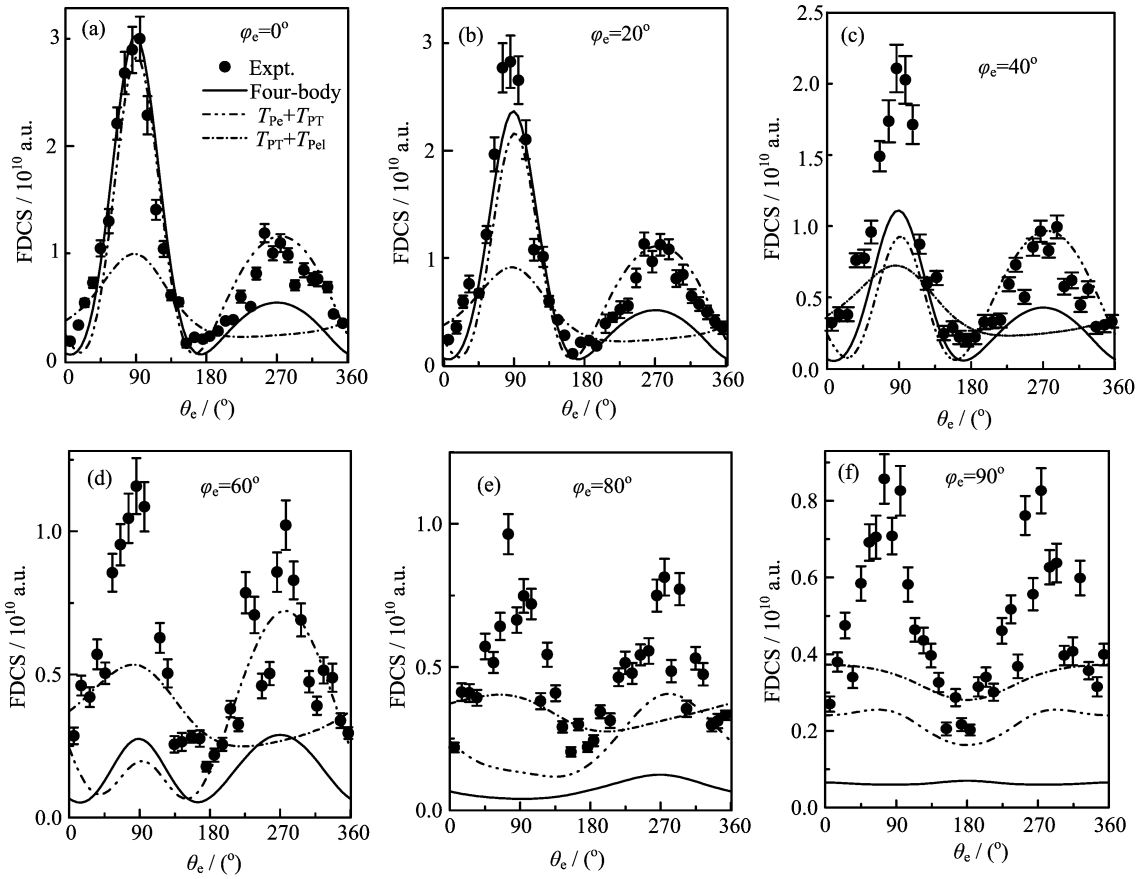

FIG. 3 The coherent sum contributions to the FDCS of the scattering amplitudes.

cross section that almost tends to experimental binary peak. When T_{Pe1} is switched on, the cross section due to the interference of the three scattering amplitudes in magnitude and width more tends to the experimental results.

It is evidently seen from Fig.2(a) that the largest individual incoherent contribution to the cross-section around the recoil region comes from the scattering amplitude T_{PT}. In Fig.3(a), it seems that the cross section around the recoil region due to interference between T_{Pe} and T_{PT} reveals a distinct peak, which is in excellent agreement with experimental recoil peak. This suggests that the electron first undergoes a binary collision with the projectile and then gets backscattered by the target nucleus. In addition, the coherent contributions of amplitude T_{Pe1} influence the magnitude and width of the recoil peak.

As φ_e increases (Fig.2 (b)−(f)), around binary peak, the contribution to the cross-section from the scattering amplitude T_{Pe} gradually decreases but the contribution from T_{PT} gradually increases. From φ_e=60° to 90° (Fig.2 (d)−(f)), the largest individual incoherent contribution to the cross-section comes from the scattering amplitude T_{PT}. It is evidently that the projectile-target nucleus interaction (PT) plays a significant role in the observed cross sections, which is different from a very recent theoretical result [5]. In Fig.3 (b)−(e), as φ_e is increased, though the individual incoherent contribution from T_{Pe1} keeps the smallest around binary peak, the major coherent contribution to the cross-sections arising from $T_{P,core}$ dominates over interference between T_{PT} and T_{Pe}.

For recoil peak, the largest separate contribution to the FDCS always comes from the scattering amplitude T_{PT} in any geometry (Fig.2). Although partial cross sections arising from T_{PT} do not present the recoil peak structure at all, the cross sections due to the interference between T_{PT} and T_{Pe} basically reproduce experimental results (Fig.3). However, the coherent sum of all the three scattering amplitudes makes the magnitudes of the recoil peak smaller than that of the peak arising from interference between T_{PT} and T_{Pe}.

In the perpendicular plane, the dominant contribution to cross-section around the binary and recoil regions comes from the scattering amplitude T_{PT} (Fig.2(f)). It is similar to the case of proton impact ionization (*e.g.*, [11] and references therein). Although the cross-section yielded by T_{PT} correctly predicts the position of a minimum at θ_e=180°, it only reveals a broad peak at about θ_e=0° (360°). Thus, the experi-

DOI:10.1063/1674-0068/27/03/279-284

mental results are basically qualitatively reproduced by the cross-sections arising from $T_{\rm PT}$. The partial cross-sections coming from $T_{\rm P,core}$ (Fig.3(f)) and $T_{\rm PT}$ have similar structures. More importantly, in spite that the cross-section originating from interference between $T_{\rm PT}$ and $T_{\rm Pe}$ underestimates the magnitude of the peak, it displays a double-peak structure at $\theta_{\rm e}$=90°, 270°, quite similar to that found in the experimental peak. But this feature could not be presented by the interference of the three amplitudes, which is in conflict with measurements. The failure of the four-body model predicting the feature in this geometry might has been traced back to a wrong weighting of the amplitudes $T_{\rm PT}$, $T_{\rm Pe}$, and $T_{\rm Pe1}$.

IV. CONCLUSION

Four-body model has been applied to the calculations of FDCS for single ionization of helium at impact energy of 100 MeV/amu. In geometries, except for $\varphi_{\rm e}$=80° and $\varphi_{\rm e}$=90° we find that there is a qualitative agreement between the four-body method and the measurements, but the discrepancies still present. In the scattering plane, the four-body, 3DW and FBA models are in reasonable agreement with experiment for binary peak. However, theoretical results underestimate the recoil peak of experimental cross section. As the angle $\varphi_{\rm e}$ is increased to 90°, including the four-body model, the deviation of the theoretical results from the measurements including the four-body model rises. The worst case is observed in the perpendicular plane, there is a considerable discrepancy between theoretical results and experimental data.

We have also discussed the contributions of various scattering amplitudes to FDCS in the present model. It is found that the interference effect depends sensitively on the detected geometry. As $\varphi_{\rm e}$ increases, except for $\varphi_{\rm e}$=90°, the coherent contribution to the cross-sections arising from the coherent sum of the projectile-target nucleus and projectile-passive electron interactions is larger than interference of the scattering amplitudes between projectile-target nucleus interaction and projectile-ejected electron interaction around binary peak. Furthermore, in geometries the recoil peaks were yielded by the interference of the scattering amplitudes between projectile-target nucleus interaction and projectile-ejected electron interaction. Whereas in the perpendicular plane, the experimental FDCS is not reproduced by the interference of the three amplitudes. A possible reason is an inappropriate weighting of the three amplitudes. In addition, the discrepancies between theory and experiment could be due to the possibility that the projectile beam is not coherent (Ref.[18] and references therein). Generally, there is a strong disagreement between the present theory and measurements in the perpendicular plane, so a more definitive explanation needs to be further studied, this is also our future work to be done.

V. ACKNOWLEDGMENTS

This work was supported by the National Natural Science Foundation of China (No.11274215), the Natural Science Foundation of Shanxi Province, China (No.20051008 and No.2010011009), and the Technology Project of Shanxi Provincial Education Department, China (No.20111011).

[1] K. Schneider, M. Schulz, X. Wang, A. Kelkar, M. Grieser, C. Krantz, J. Ullrich, R. Moshammer, and D. Fischer, Phys. Rev. Lett. **110**, 113201 (2013).
[2] R. Hubele, A. LaForge, M. Schulz, J. Goullon, X. Wang, B. Najjari, N. Ferreira, M. Grieser, V. L. B. de Jesus, R. Moshammer, K. Schneider, A. B. Voitkiv, and D. Fischer, Phys. Rev. Lett. **110**, 133201 (2013).
[3] M. Schulz, R. Moshammer, D. Fischer, H .Kollmus, H. D. Madison, S. Jones, and J. Ullrich, Nature **48**, 422 (2003).
[4] H. R. J. Walters and C. T. Whelan, Phys. Rev. A **85**, 062701 (2012).
[5] I. B. Abdurakhmanov, I. Bray, D. V. Fursa, A. S. Kadyrov, and A. T. Stelbovics, Phys. Rev. A **86**, 034701 (2012).
[6] A. L. Harris, D. H. Madison, J. L. Peacher, M. Foster, K. Bartschat, and H. P. Saha, Phys. Rev. A **75**, 032718 (2007).
[7] D. Madison, M. Schulz, S. Jones, M. Foster, R. Moshammer, and J. Ullrich, J. Phys. B **35**, 3297 (2002).
[8] M. McGovern, D. Assafrão, J. R. Mohallem, C. T. Whelan, and H. R. J. Walters, Phys. Rev. A **81**, 042704 (2010).
[9] J, Colgan, M. S. Pindzola, F. Robicheaux, and M. F. Ciappina, J. Phys. B **44**, 175205 (2011).
[10] X. F. Jia, S. Y. Sun, X. Y. Miao, and J. F. Zhang, Europhys. Lett. **84**, 13001 (2008).
[11] X. Y. Ma, X. Li, S. Y. Sun, and X. F. Jia, Europhys. Lett. **98**, 53001 (2012).
[12] X. Li, X. Y. Ma, S. Y. Sun, and X. F. Jia, Chin. Phys. B **21**, 113403 (2012).
[13] F. W. Byron and C. J. Joachain, Phys. Rev. **146**, 1 (1966).
[14] M. Brauner, J. S. Briggs, and H. Klar, J. Phys. B **22**, 2265 (1989).
[15] J. Berakdar, J. S. Briggs, and H. Klar, J. Phys. B **26**, 285 (1993).
[16] J. Berakdar, J. S. Briggs, and H. Klar, Z. Phys. D **24**, 351 (1992).
[17] M. Schulz, B. Najjari, A. B. Voitkiv, K. Schneider, X. Wang, A. C. Laforge, R. Hubele, J. Goullon, N. Ferreira, A. Kelkar, M. Grieser, R. Moshammer, J. Ullrich, and D. Fischer, Phys. Rev. A **88**, 022704 (2013).
[18] X. Wang, K. Schneider, A. LaForge, A. Kelkar, M. Grieser, R. Moshammer, J. Ullrich, M. Schulz, and D. Fischer, J. Phys. B **45**, 211001 (2012).

DOI:10.1063/1674-0068/27/03/279-284